

## Low Threshold Operation of Tensile Strained InGaAs/InGaAsP Quantum Well Lasers with Simple Separate-Confinement Heterostructures

Tsuyoshi YAMAMOTO, Hiroyuki NOBUHARA, Mitsuru SUGAWARA,  
Takuya FUJII, and Kiyohide WAKAO

Fujitsu Laboratories Ltd.

10-1, Morinosato-Wakamiya, Atsugi 243-01, Japan

We investigated tensile strained InGaAs/InGaAsP quantum well lasers with simple separate-confinement heterostructures (SCH). We obtained a threshold current below 2 mA at 20°C with an indium mole fraction of the active layers between 0.3 and 0.4. We found that the InGaAsP composition of barrier and SCH layers plays an important role in determining temperature characteristics. Using a carefully chosen composition of the SCH layer, we obtained 1.6 mA CW-threshold currents at 20°C and lasing at as high as 120°C.

### 1. Introduction

Long wavelength semiconductor lasers which operate at low threshold current make zero bias modulation possible in local area network and optical interconnection applications. Low threshold operation of tensile strained quantum well lasers has been demonstrated experimentally.<sup>1,2)</sup> In strained quantum well lasers, a separate-confinement heterostructure (SCH) greatly affects the laser characteristics, because the SCH determines the optical and carrier confinement to the quantum wells. There are two types of SCH, one is graded-index (GRIN), the other is single-step SCH. Previous studies used multi-step GRIN-SCH.<sup>1,2)</sup> Studies of low threshold operation of tensile strained quantum well lasers have not thoroughly investigated the single-step SCH.

In this paper, we report low threshold operation of tensile strained InGaAs/InGaAsP quantum well lasers with a single-step SCH.

### 2. Device structures and fabrication

We fabricated tensile strained quantum well lasers with indium mole fraction ( $x$ ) of quantum wells between 0.2 and 0.4. The thickness ( $L_w$ ) and the number ( $N_w$ ) of the wells are summarized in Fig. 1 with a schematic band diagram. The barrier and SCH layers have the same InGaAsP composition, that is, they form a single-step SCH. This is the simplest possible SCH. Because there are less heterointerfaces than more complex SCH structures, there may be less deterioration of lasing characteristics due to nonradiative recombination at heterointerfaces. To investigate the influence of the composition of the SCH layer ( $\lambda_{SCH}$ ), we used 1.1 and 1.2  $\mu\text{m}$  composition InGaAsP.

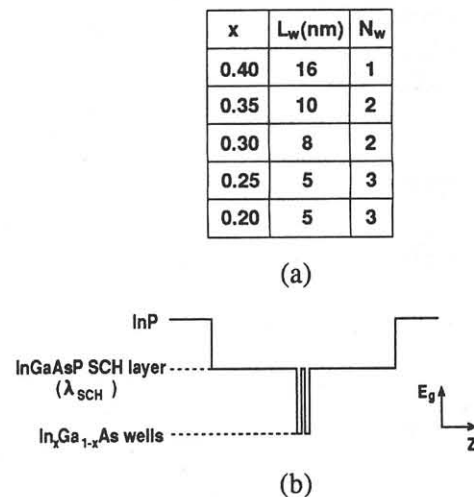


Figure 1 Structures of fabricated lasers. (a) Structure parameters of active layers. (b) Schematic band diagram.

We determined a thickness of SCH layer to maximize optical confinement to quantum wells for each InGaAsP composition. The thickness of the barrier layer was 10 nm.

We grew these strained quantum well layers on n-doped InP (100) substrates by low pressure MOVPE.<sup>3)</sup> We then formed a flat-surface buried heterostructure (FBH) using two-step LPE growth.<sup>4)</sup> Lasers were cleaved into 200-1500  $\mu\text{m}$  lengths. Both facets of the 200  $\mu\text{m}$  long lasers were high-reflection (HR) coated ( $R_f = R_r = 92\%$ ) for low threshold current operation. Laser chips were mounted on diamond heatsinks in the p-side-up configuration.

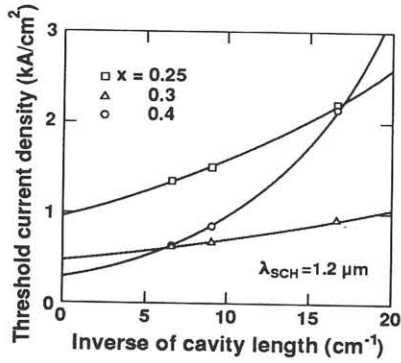


Figure 2 Cavity length dependence of threshold current density of the lasers with  $x = 0.25, 0.3,$  and  $0.4$  with a  $1.2 \mu\text{m}$  composition InGaAsP SCH layer.

### 3. Device characteristics

We measured static characteristics under CW operation. The light output of these lasers was all TM-polarized.

We plotted the dependence of threshold current density on cavity length of lasers with  $x=0.25, 0.3,$  and  $0.4$  with a  $1.2 \mu\text{m}$  composition SCH layer (Fig. 2). We calculated threshold current density by dividing the threshold current by the active layer area ignoring the leak current of the FBH structure. For  $x=0.4$ , the threshold current density rapidly increased as cavity length decreased. This is because the thick well causes the gain saturation from lower current density. The different threshold current density at infinite cavity length is mainly because of the different number of wells. Assuming a logarithmic relationship between gain and current density, we estimated the threshold current density per well at infinite cavity length to be  $320 \text{ A/cm}^2$  for  $x = 0.25$ ,  $240 \text{ A/cm}^2$  for  $x = 0.3$ , and  $290 \text{ A/cm}^2$  for  $x = 0.4$ . Threshold current density per well at infinite cavity length has a minimum at around  $x = 0.3$ . We believe this is from the relationship between the modification of valence band structure and the deterioration of crystal quality due to strain. This tendency was

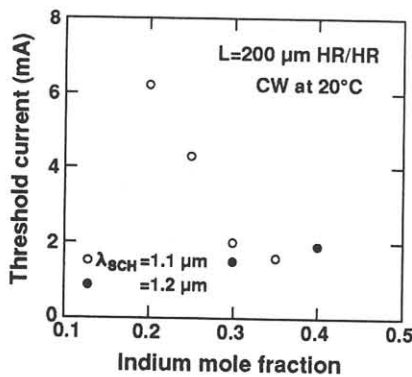
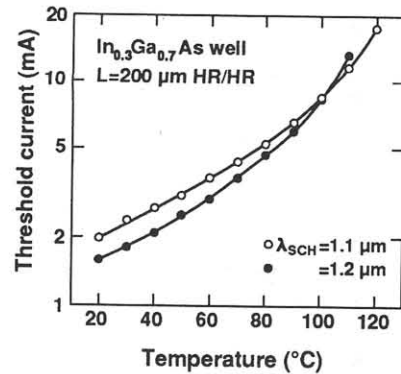


Figure 3 CW threshold current at  $20^\circ\text{C}$  on each indium mole fraction of active layers.

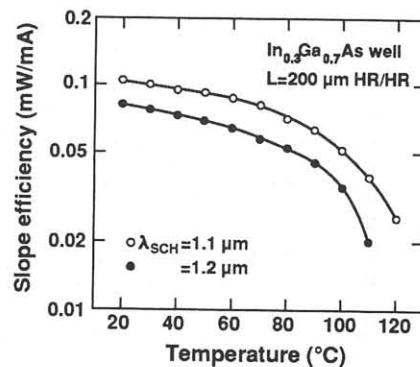
observed in a previous report <sup>2)</sup> and for a larger strain ( $x=0.25$ ), a lower value was obtained.

Threshold currents at  $20^\circ\text{C}$  of HR coated devices which are  $200 \mu\text{m}$  long are shown in Fig. 3. We obtained threshold currents below  $2 \text{ mA}$  for  $x$  between  $0.3$  and  $0.4$ . The minimum threshold current was  $1.5 \text{ mA}$  for the laser with  $x = 0.3$  and a  $1.2 \mu\text{m}$  composition SCH. This value is comparable to  $1.0 \text{ mA}$  for a  $150 \mu\text{m}$  long device. <sup>2)</sup> Even in the large-strain region ( $x = 0.2$ ), the threshold current was a  $6.2 \text{ mA}$ .

We plotted temperature dependence of threshold current of the lasers with two  $\text{In}_{0.3}\text{Ga}_{0.7}\text{As}$  wells with a  $1.1$  and  $1.2 \mu\text{m}$  composition SCH layer (Fig. 4 (a)). At around room temperature the laser with a  $1.2 \mu\text{m}$  composition SCH had a lower threshold current than that with a  $1.1 \mu\text{m}$  composition SCH. This difference is a result of the different optical confinements in the quantum wells. The characteristic temperature  $T_0$  between  $20^\circ\text{C}$  and  $50^\circ\text{C}$  was  $68\text{K}$  for a  $1.1 \mu\text{m}$  composition SCH and  $67\text{K}$  for a  $1.2 \mu\text{m}$  composition SCH. These values were greater by  $15\text{-}20\text{K}$  than values reported for low threshold GRIN-SCH tensile strained quantum well lasers. <sup>1,2)</sup> Around room temperature, the composition of SCH has little effect on



(a)



(b)

Figure 4 Temperature characteristics of the  $\text{In}_{0.3}\text{Ga}_{0.7}\text{As}$  two quantum wells lasers with an SCH composition of  $1.1$  and  $1.2 \mu\text{m}$ . (a) Threshold current. (b) Slope efficiency.

$T_0$ . At higher temperatures, however, the laser with a 1.2  $\mu\text{m}$  composition SCH showed a poorer temperature characteristic despite its lower threshold current.  $T_0$  between 50°C and 80°C was 56K for a 1.1  $\mu\text{m}$  composition SCH and 48K for a 1.2  $\mu\text{m}$  SCH. Above 100°C, the laser with a 1.1  $\mu\text{m}$  composition SCH had a lower threshold current.

We believe this difference is a result of the different carrier confinements in the quantum wells. Carrier is confined by the energy difference between barrier and well layer. Therefore, for a longer band-gap wavelength composition of an SCH layer, there is more carrier overflow into the SCH layer from a well at high temperature when there are many carriers with high energy. Carrier overflow follows the increase in recombination current in the SCH layer and the absorption loss of the SCH layer due to free carrier absorption and inter-valence band absorption. This raises the threshold current. This shows that carrier confinement to the quantum wells plays an important role in deciding the temperature characteristic. This is in addition to the generally stated reasons, that is, gain characteristics,

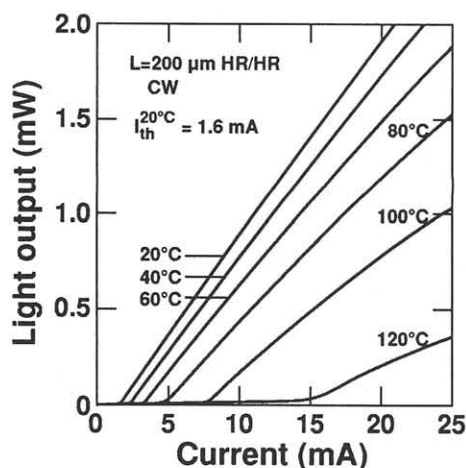


Figure 5 CW light-current characteristic of the tensile strained  $\text{In}_{0.35}\text{Ga}_{0.65}\text{As}$  two quantum wells laser with an SCH composition of 1.1  $\mu\text{m}$ . The lasing wavelength was 1.48  $\mu\text{m}$  at 20°C.

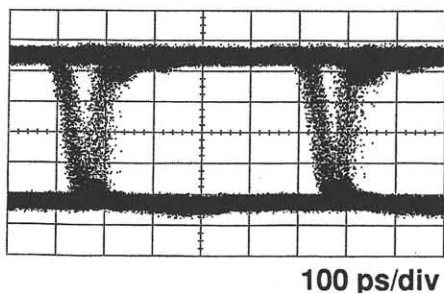


Figure 6 The eye pattern under zero-bias modulation (2Gbit/s) at 20°C. The driving current was 40 mA.

Auger recombination, and inter valence band absorption. The temperature dependence of slope efficiency is shown in Fig. 4 (b). A laser with a 1.1  $\mu\text{m}$  composition SCH has a larger slope efficiency and better temperature characteristic because the SCH layer has a smaller absorption coefficient and less carrier overflow. Therefore, for high temperature operation, it is important to optimize the composition of barrier and SCH layers to obtain a sufficient carrier confinement.

Fig. 5 shows the CW light output-current characteristics of a laser with  $x=0.35$  and a 1.1  $\mu\text{m}$  composition SCH layer. The threshold current was 1.6 mA at 20°C and we achieved lasing at as high as 120°C. We attempted zero-bias modulation with this laser and measured the eye pattern at 2Gbit/s NRZ modulation at 20°C (Fig. 6). The large eye opening suggests that this laser can be used for high-speed modulation at zero-bias.

#### 4. Summary

We have demonstrated that simple SCH structures are sufficient for low threshold operation of tensile strained  $\text{InGaAs/InGaAsP}$  quantum well lasers. The composition of the SCH layer was found to affect the temperature characteristics. Using a carefully chosen SCH layer composition, we obtained a 1.6 mA CW threshold current at 20°C and lasing at up to 120°C.

#### Acknowledgements

We would like to thank Drs. H. Imai and S. Yamazaki for their encouragement during this work, and Messrs. K. Tanaka, T. Odagawa, T. Inoue, and T. Machida for helpful advice and assistance with experiments.

#### References

- 1) C. E. Zah, R. Bhat, B. Pathak, C. Caneau, F. J. Favire, N. C. Andreadakis, D. M. Hwang, M. A. Koza, C. Y. Chen, and T. P. Lee, *Electron. Lett.* **27** (1991) 1414.
- 2) P. J. A. Thijs, J. J. M. Binsma, L. F. Tiemeijer, and T. van Dongen, *Electron. Lett.* **28** (1992) 829.
- 3) M. Kondo, J. Okazaki, H. Sekiguchi, T. Tanahashi, S. Yamazaki, and K. Nakajima, *J. Cryst. Growth*, **115** (1991) 231.
- 4) K. Wakao, K. Kihara, Y. Kotaki, T. Kusunoki, H. Sudo, S. Isozumi, S. Yamakoshi, H. Ishikawa, and H. Imai, *J. Appl. Phys.* **62** (1987) 2153.